

# Study of $\text{PbZr}_{0.53}\text{Ti}_{0.47}\text{O}_3$ solid solution formation by interaction of perovskite phases

Ľ. Medvecký<sup>a,\*</sup>, M. Kmecová<sup>a</sup>, K. Saksl<sup>b</sup>

<sup>a</sup> Institute of Materials Research of SAS, Watsonova 47, 04353 Kosice, Slovakia

<sup>b</sup> HASYLAB am Deutschen Elektronen Synchrotron, DESY, Notkestrasse 85, D-22603 Hamburg, Germany

Received 9 January 2006; received in revised form 9 May 2006; accepted 20 May 2006

Available online 28 July 2006

## Abstract

The formation of  $\text{Pb}(\text{Zr}_{0.53}\text{Ti}_{0.47})\text{O}_3$  solid solution around the MPH was studied by mutual interaction of perovskite PZT phases (rhombohedral and tetragonal) and by interaction of PZT phases with  $\text{PbTiO}_3$  or  $\text{PbZrO}_3$  at sintering temperature. Starting perovskite phases were prepared by the mechanical homogenization of oxidic precursors and calcination of mixtures at 1000 °C. The final  $\text{Pb}(\text{Zr}_{0.53}\text{Ti}_{0.47})\text{O}_3$  ceramic systems prepared from perovskite mixtures were monophasic (tetragonal symmetry) in comparison with the biphasic ceramics prepared from calcinate with the same stoichiometry. The magnitude of deviation from equilibrium chemical composition or fluctuation from final stoichiometry in PZT phase in starting powder perovskite mixtures was not crucial for the formation of monophasic  $\text{Pb}(\text{Zr}_{0.53}\text{Ti}_{0.47})\text{O}_3$  ceramic system prepared using such a method. © 2006 Elsevier Ltd. All rights reserved.

**Keywords:** PZT; Perovskites; Powders-solid state reaction

## 1. Introduction

$\text{Pb}(\text{Zr}_x\text{Ti}_{1-x})\text{O}_3$  (PZT) solid solutions with composition very close to the morphotropic phase boundary (MPH) ( $x=0.53$ ) represent materials with useful ferroelectric and piezoelectric properties which make them useful as transducers and other piezoelectric devices. The phase diagram<sup>1</sup> of PZT system originally contained four different types of phases- two rhombohedral phases in region with higher Zr content (low- and high-temperature phases), the tetragonal phase on the side of higher Ti content and the cubic phase above the Curie temperature (Fig. 1). The tetragonal and rhombohedral region were sharply separated one from another by the MPH. In most references focused on the preparation of PZT systems, the coexistence of rhombohedral and tetragonal phases at MPH was found as the result of the formation of various types of fluctuations in preparation process. The monoclinic phase has been found in samples with composition near MPH, which separates rhombohedral and tetragonal region in phase diagram,<sup>2</sup> as the high resolution XRD measurements (HRXRD) of extremely homogeneous samples

showed. Detailed phase analysis showed that both tetragonal and monoclinic phases were present in PZT systems at intermediate temperatures whereas the mixture of monoclinic and rhombohedral phases was not observed.<sup>3</sup> According to the statistical distribution model,<sup>4</sup> in which a two phase PZT system with composition close to MPH (tetragonal and rhombohedral phases) is created at room temperature as the result of thermal fluctuations during cooling, the width of the coexistence region (WCR) is inversely proportional to the volume of the element in a statistical ensemble, thus, the particle size in a powder system. The lower crystal size in ceramic samples induces inhomogeneous internal stress and the tetragonal-rhombohedral system is created. The formation of monoclinic phase is inhibited under such conditions. Thermodynamic models point out the possibility of the coexistence of the tetragonal and rhombohedral phases around the MPH as a consequence of the presence of chemical heterogeneities in PZT system.<sup>5,6</sup> Early observations that confirmed the existence of a solubility gap between the tetragonal and rhombohedral phases, in which the lattice parameters of the phases did not change with composition ( $x$ ),<sup>7</sup> were not verified by precise XRD measurements.<sup>3,8</sup> Similarly, PZT systems prepared by the wet-dry combination technique were monophasic.<sup>9</sup> This fact is inconsistent with the above model. Measurements of dependences of dielectric properties on composition of PZT sys-

\* Corresponding author.

E-mail address: [imedvecky@imr.saske.sk](mailto:imedvecky@imr.saske.sk) (Ľ. Medvecký).

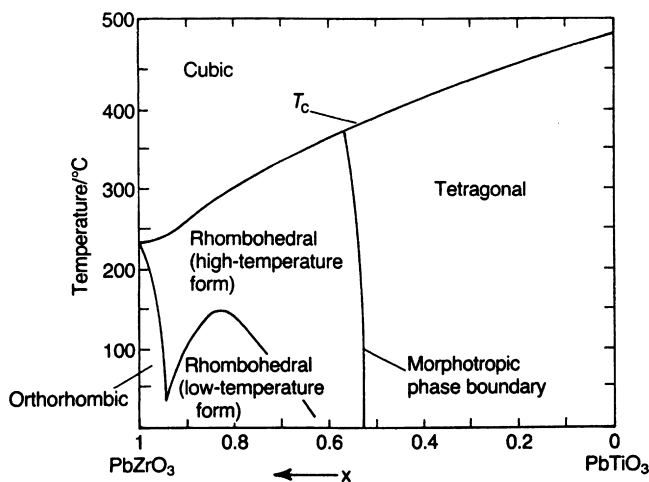


Fig. 1. Phase diagram of PZT system (Jaffe et al.<sup>1</sup>).

tems and their detailed analysis showed that the WCR depends on particle size in PZT system.<sup>8</sup> This result supports the statistical distribution model. On the other hand, the formation of biphasic PZT systems, which was found in samples prepared by the sol–gel process after high-temperature treatment, was connected with fluctuations in chemical compositions and need not be explained on the basis of thermal fluctuations.<sup>10,11</sup> A significant influence on the phase composition of PZT system near the MPH is brought about by PbO excess. With the rise of PbO content in the PbO–PZT system, the content of rhombohedral phase increases according to the phase diagram of this system.<sup>12</sup> The WCR decreased with both the PbO excess and the calcination temperature of PbO–PZT system.<sup>13</sup> This effect was probably caused by the presence of a liquid phase during calcination. The decrease in WCR with sintering temperature and dopant concentration was observed in doped PZT systems too.<sup>14,15</sup>

In this paper, the formation of  $\text{Pb}(\text{Zr}_{0.53}\text{Ti}_{0.47})\text{O}_3$  solid solution with composition around the MPH was studied by the mutual interaction of perovskite PZT phases (rhombohedral and tetragonal) and by interaction of PZT phases with  $\text{PbTiO}_3$  or  $\text{PbZrO}_3$ . This procedure makes it possible to determine the influence of starting chemical and phase fluctuations on final composition of PZT ceramics, WCR and the creation of the two phase system near the MPH.

## 2. Experimental procedure

PZT and  $\text{PbZrO}_3$  (or  $\text{PbTiO}_3$ ) phases were prepared by mechanical homogenization of powder precursors  $\text{PbCO}_3$  (analytical grade),  $\text{TiO}_2$  and  $\text{ZrO}_2$  (>99%) in a ball mill (agate balls and PE vessel) in methanol for 15 h. After drying, final oxide mixtures were calcined at 1000 °C for 1 h in air. Mutual interactions of perovskite phases –  $\text{Pb}(\text{Zr}_{0.5}\text{Ti}_{0.5})\text{O}_3$  (tetragonal symmetry),  $\text{Pb}(\text{Zr}_{0.6}\text{Ti}_{0.4})\text{O}_3$  (rhombohedral symmetry),  $\text{PbZrO}_3$  and  $\text{PbTiO}_3$  – were studied in biphasic powder mixtures of these phases prepared by mechanical homogenization of two powder perovskite phases in a ball mill for 15 hours in methanol. PZT phases were combined in order to obtain PZT ceramics with  $\text{Pb}(\text{Zr}_{0.53}\text{Ti}_{0.47})\text{O}_3$  final stoichiometry. Dried

mixtures were pressed into pellet form (13 mm diameter and 2 mm height). Pellets were sintered at 1200 °C for 1 h in a closed  $\text{Al}_2\text{O}_3$  crucible. The pellets during sintering were covered with the PZT mixture from which each one was prepared.

In situ XRD temperature measurements of powder PZT mixtures were done in transmission mode with collimated synchrotron radiation of photon energy 79.9 keV ( $\lambda = 0.155236 \text{ \AA}$ ). The XRD patterns were recorded by a 2D detector (mar345 Image plate) and integrated to  $2\theta$  space by using the program Fit2D.<sup>19</sup> Spectra were collected at every 50 °C up to temperature of 780 °C (maximal possible temperature which can be achieved in the used device) at a heating rate of 100 °C/min. and pressure of 10 mbar. From the temperature of 780 °C, the samples were rapid cooled down to room temperature and the XRD spectrum of the sample was recorded.

High-resolution XRD measurements of the powder samples were done in a quartz capillary and the samples were illuminated by monochromatic synchrotron radiation of photon energy 100.012 keV ( $\lambda = 0.155236 \text{ \AA}$ ). Spectra were collected in high-resolution transmission mode with  $2\theta$  step intervals of 0.003° for 2 s. XRD profile was measured using Ge-semiconductor detector with Si(1 1 1) crystal analyzer.

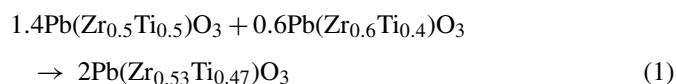
XRD diffraction measurements were performed using XRD diffractometer (X'Pert Pro Philips) with Cu K $\alpha$  radiation and scan step size of 0.0167°.

Microstructures of fractured PZT ceramic samples were observed by scanning electron microscopy (SEM, TESLA BS 340).

## 3. Results and discussion

In Fig. 2a–c, XRD diffraction spectra of PZT calcinates prepared at 1000 °C are shown. The changes in the phase composition and the formation of PZT systems prepared by the reaction of oxidic precursors can be visible in spectra. The comparison of XRD diffraction records confirms previously found results, that rhombohedral phase is detected in  $\text{Pb}(\text{Zr}_x\text{Ti}_{1-x})\text{O}_3$  systems (systems prepared by similar method) with increasing of Zr content ( $x > 0.5$ ) and two phase rhombohedral–tetragonal system is created. Simultaneously, the lattice parameter  $a$  of tetragonal phase rise with Zr content in these systems (see Table 1). In Table 1, lattice parameters of  $P4mm$  tetragonal phase were determined by the Rietveld analysis of XRD spectra using LHPM program.<sup>16</sup> Rhombohedral and tetragonal phases are clearly visible at  $x = 0.53$ , which corresponds to composition close to MPB.

HR XRD diffractograms of mixtures prepared by the homogenization of various perovskite phases are shown in Fig. 3. Spectrum 1 represents mixture according to following equation:



where  $\text{Pb}(\text{Zr}_{0.5}\text{Ti}_{0.5})\text{O}_3$  has tetragonal symmetry (the content of rhombohedral phase <2 vol.%—no peaks were found in XRD spectrum in Fig. 2, curve 4) and  $\text{Pb}(\text{Zr}_{0.6}\text{Ti}_{0.4})\text{O}_3$  (Fig. 2, curve 7) has rhombohedral symmetry. Mixtures (2) and (3) were prepared

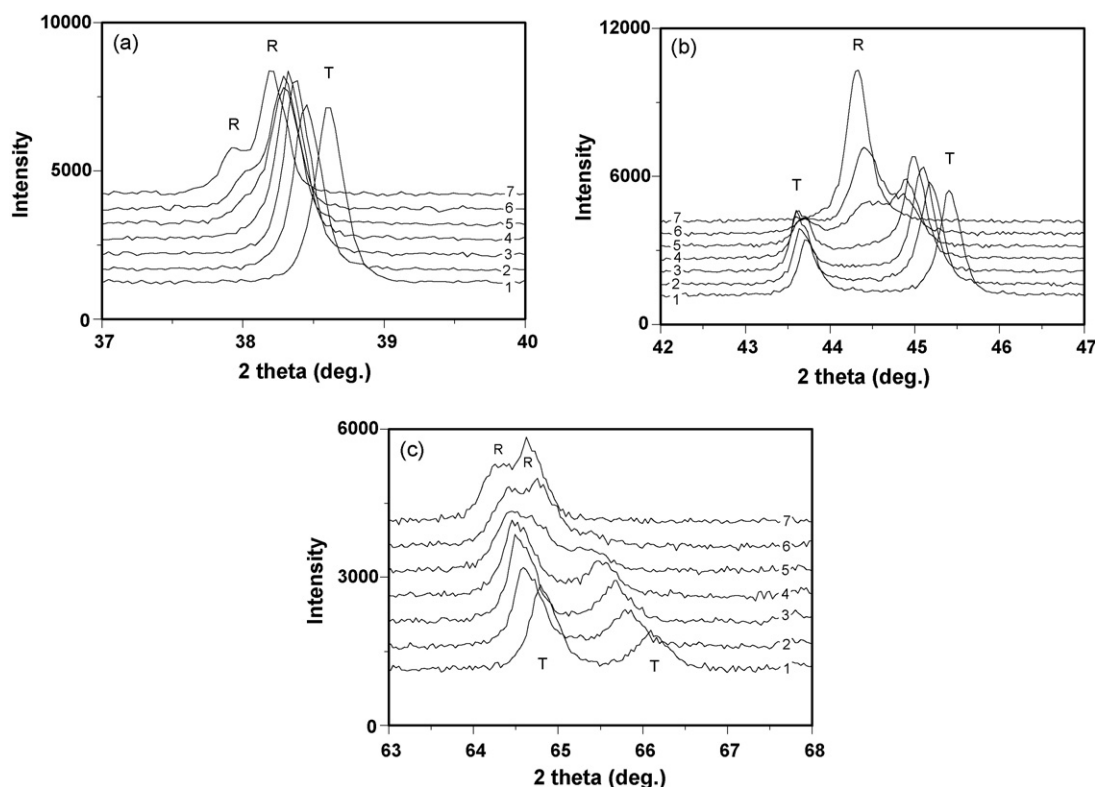


Fig. 2. XRD diffraction spectra of PZT calcinates prepared at 1000 °C: (a) (1 1 1) reflection, (b) (2 0 0) reflections and (c) (2 2 0) reflections from planes of pseudocubic PZT phase. (1) Zr/Ti = 0.4/0.6; (2) Zr/Ti = 0.45/0.55; (3) Zr/Ti = 0.47/0.53; (4) Zr/Ti = 0.5/0.5; (5) Zr/Ti = 0.53/0.47; (6) Zr/Ti = 0.55/0.45; (7) Zr/Ti = 0.6/0.4.

as follows:

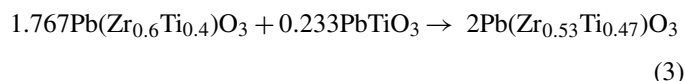
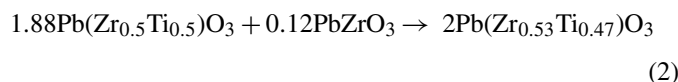


Table 1

Values of  $a$  and  $c$  lattice parameters of tetragonal phase in PZT calcinates (prepared by reaction of mixture of oxides) and in PZT ceramics (prepared from mixtures of perovskite phases; standard represents PZT ceramics prepared from calcinate 5)

	Ratio of Zr/Ti	Lattice parameters of tetragonal phase $a/c$ (nm)	$R_{wp}$ (%)	$R_b$ (%)
<b>Calcinates</b>				
1	0.4/0.6	0.4002/0.4146	4.8	2.2
2	0.45/0.55	0.4016/0.4145	5.6	3.0
3	0.47/0.53	0.4020/0.4145	5.6	2.9
4	0.5/0.5	0.4029/0.4142	4.9	1.7
5	0.53/0.47	0.4037/0.4134	4.8	1.3
6	0.55/0.45	0.4044/0.4129	5.1	2.6
<b>Ceramics</b>				
Standard	0.53/0.47	0.4034/0.4135	5.1	2.1
1	0.53/0.47	0.4037/0.4134	4.7	1.5
2	0.53/0.47	0.4036/0.4130	4.9	1.8
3	0.53/0.47	0.4037/0.4132	5.0	2.0

$R_{wp}$  and  $R_b$  are the agreements factors (the Rietveld analysis).

From the above equations, the fluctuations in chemical composition considering the equilibrium value  $x$  given by the chemical equations can be determined. Note, all systems were prepared from the same starting oxidic precursors, they were homogenized under the same conditions and calcined or sintered during a single temperature cycle. This procedure eliminates the formation of thermal fluctuations and fluctuations originating from a different content of impurities in the systems, which can play a significant role from the point of view of phase composition

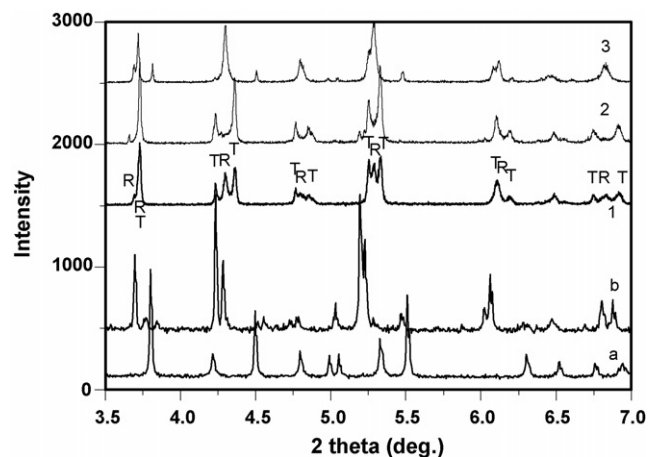


Fig. 3. HR XRD diffractograms of powder mixtures prepared by the homogenization of various perovskite phases. (1)  $\text{Pb}(\text{Zr}_{0.5}\text{Ti}_{0.5})\text{O}_3 + \text{Pb}(\text{Zr}_{0.6}\text{Ti}_{0.4})\text{O}_3$ ; (2)  $\text{Pb}(\text{Zr}_{0.5}\text{Ti}_{0.5})\text{O}_3 + \text{PbZrO}_3$ ; (3)  $\text{Pb}(\text{Zr}_{0.6}\text{Ti}_{0.4})\text{O}_3 + \text{PbTiO}_3$ ; (a)  $\text{PbTiO}_3$ ; (b)  $\text{PbZrO}_3$ . T: tetragonal phase; R: rhombohedral phase.

and the formation of two phase systems. However, the deviation from equilibrium composition could not be exactly determined in Ref. <sup>10</sup> in spite of the sol–gel preparation of the PZT systems. In mixture (1), the deviation cannot be so clearly determined because of the high content of rhombohedral (30 at.%,  $\Delta x = 0.07$ ) and tetragonal (70 at.%,  $\Delta x = 0.03$ ) phases in the mixture. Fluctuations from equilibrium composition ( $x = 0.53$ ) can be characterized by the deviation of the majority PZT phase from equilibrium stoichiometry  $-\Delta x = 0.03$  in mixture (2) and  $\Delta x = 0.07$  in mixture (3). From the above results, the lowest deviation from equilibrium composition in mixtures is 0.03 and maximal 0.07.

HR XRD diffraction patterns of ceramic samples after sintering at 1200 °C are shown in Fig. 4a and b. The sample 1 prepared from oxidic mixture (with  $x = 0.53$ ) represents two-phase tetragonal–rhombohedral system as a result of comparison of peaks from reflection of (1 1 1) (Fig. 4a) and (2 0 0), (0 0 2) (Fig. 4b) planes of pseudocubic PZT phase. Samples with the same final composition as in the sample 1 but prepared from perovskite mixtures were composed from almost pure tetragonal phase (curves 2–4 in Fig. 4). Very small additional contribution of rhombohedral phase on the composition in sample 3 (curve 4) can be verified by the insignificant extension of peak width

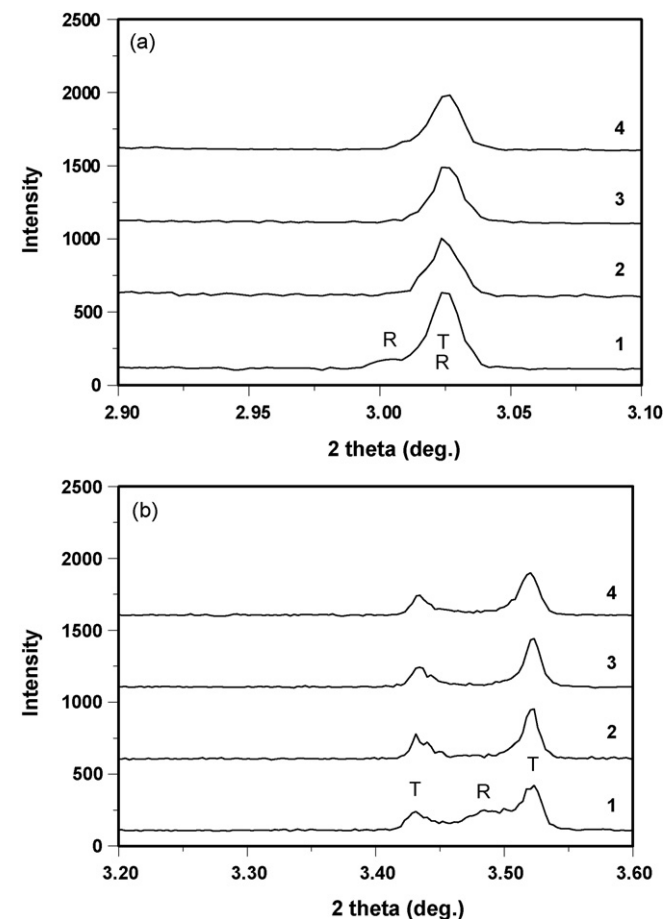


Fig. 4. HR XRD diffraction patterns of ceramic samples after sintering at 1200 °C prepared from  $\text{Pb}(\text{Zr}_{0.53}\text{Ti}_{0.47})\text{O}_3$  calcinate (spectrum 1), mixture (1) (spectrum 2), mixture (2) (spectrum 3), mixture (3) (spectrum 4). T: tetragonal phase; R: rhombohedral phase.

only. From Table 1 and comparison of peaks in Fig. 4 it is clear that values of lattice parameters  $a$ ,  $c$  of tetragonal phase are very close in all ceramic samples.

Conditions of XRD temperature measurements with fast heating up to 780 °C and rapid cooling to room temperature at lowered atmospheric pressure were selected for recording initial stages of mutual interactions. Lower pressure of ambient atmosphere replaces the low interaction temperature from the point of view of PbO partial pressure because PbO has noticeable partial pressure at high temperatures. Differences in PbO partial pressures above PZT systems and ambient atmosphere or between various PZT phases in PZT powder mixtures depend on applied temperature and the ratio of Zr/Ti in individual phases. Mutual interactions of perovskite phases are clearly visible mainly in mixtures (2) and (3) as shown in Fig. 5, where the tetragonality of major  $\text{Pb}(\text{Zr}_{0.5}\text{Ti}_{0.5})\text{O}_3$  phase in mixture (2) (Fig. 5c) and  $\text{PbTiO}_3$  content in mixture (3) (Fig. 5d) decrease. In XRD spectra of mixtures (2) and (3) after thermal cycle, a small peak around  $2\theta \sim 3^\circ$  was found. This peak corresponds to the position of a  $\text{PbZrO}_3$  peak shifted to higher angles which can be caused by the partially substitution of Zr ions by Ti ions in  $\text{PbZrO}_3$  lattice. In the spectrum of mixture (3) (the interaction of PZT phase with  $\text{PbTiO}_3$ ), this peak was not observed.

Interactions between  $\text{PbZr}_{0.53}\text{Ti}_{0.47}\text{O}_3$  phase (curves 5 in Fig. 2) and  $\text{TiO}_2$  or  $\text{ZrO}_2$  (2 or 5 wt.% excess) at sintering temperature of 1200 °C can be described on the basis of the analysis of XRD diffraction records of ceramic samples (Fig. 6a and b). From XRD spectra, it is clear that dissolution and mutual interaction of  $\text{ZrO}_2$  with PZT phase were not significant and  $\text{ZrO}_2$  remains in ceramics practically in its origin state as a secondary phase. Any change in phase composition of PZT phase and peak shift in its XRD patterns were found after sintering. On the other hand, the strong interaction of  $\text{TiO}_2$  with PZT phase and transformation of biphasic PZT system to monophasic tetragonal system were observed under the given preparation conditions. Both the tetragonality increase with  $\text{TiO}_2$  excess and the segregation of  $\text{ZrO}_2$  can be visible in the XRD records (Fig. 6a) whereas the  $\text{ZrO}_2$  content rises with  $\text{TiO}_2$  excess in PZT system after thermal process. Thus, the  $\text{TiO}_2$  excess in PZT system causes segregation of  $\text{ZrO}_2$  from native stoichiometric PZT system and the formation of PZT system with different stoichiometry (lowered  $x$ ). From this it follows that pure  $\text{ZrO}_2$  or PZT phases with high Zr content will interact as the last in nonstoichiometric (or temporarily chemically nonequilibrium, e.g., not fully reacted) systems. Such an interaction process can be explained by the rise of thermal stability in newly formed PZT system in which high temperature PbO partial pressure is lower than in original system with higher Zr content.<sup>17</sup>

Microstructures of all PZT ceramics were very similar and average particle size was about 4  $\mu\text{m}$  (Fig. 7).

The presence of a small peak representing partial Ti substituted  $\text{PbZrO}_3$  phase verifies more intensive decomposition of one of the phases in mixtures (1) and (2) during thermal treatment. In mixture (2) (Fig. 5c), where the tetragonal PZT system interacts with the pure  $\text{PbZrO}_3$  phase,  $\text{PbZrO}_3$  peaks in XRD spectrum were shifted to higher angles as the consequence of the diffusion of Ti ions into  $\text{PbZrO}_3$  lattice. This fact confirms

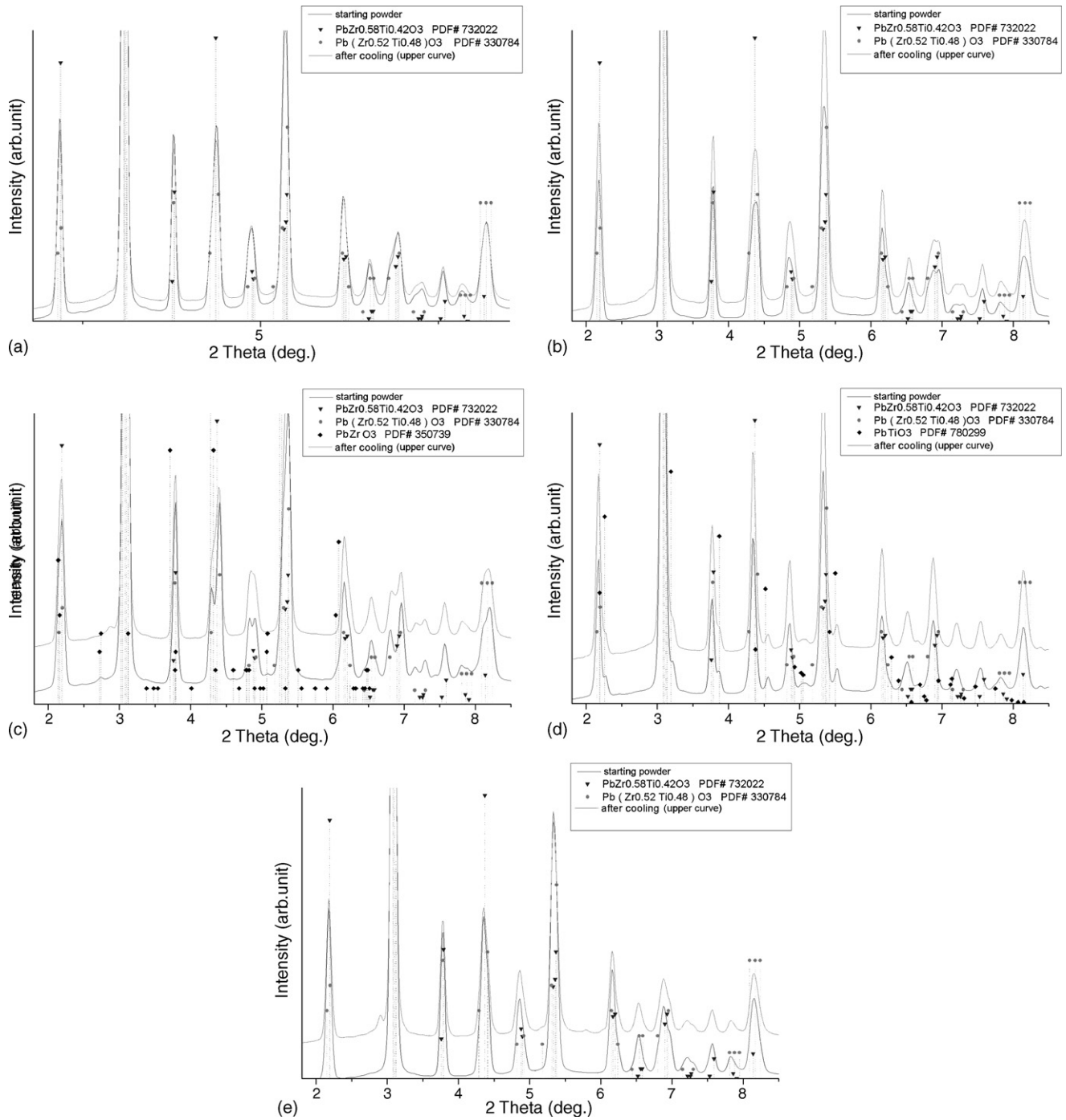


Fig. 5. XRD temperature measurements of powder mixtures with fast heating up to 780 °C and rapid cooling to room temperature at lowered atmospheric pressure. (a)  $\text{Pb}(\text{Zr}_{0.53}\text{Ti}_{0.47})\text{O}_3$  calcinate; (b) mixture (1); (c) mixture (2); (d) mixture (3); (e) tetragonal and rhombohedral phase mixture ( $x=0.55$  in final PZT ceramics) with approximately double amount of rhombohedral phase as in mixture (1).

practically the same height of  $\text{PbZrO}_3$  peaks and hence the volume fraction of this phase in mixture. Interaction is relatively intensive which as seen from the tetragonality decrease in the PZT phase. The reason for the stability of the tetragonal phase in the final PZT system ( $x=0.53$ ) could be the high initial fraction of tetragonal phase in the mixture and the small deviation ( $\Delta x=0.03$ ) of  $x$  from equilibrium stoichiometric final composition of this phase after annealing. Such an explanation conflicts with the opposite case as can be seen in mixture (3), where the

final PZT phase has tetragonal symmetry in spite of the presence of a high fraction of the rhombohedral phase in mixture. High  $\text{PbO}$  partial pressure in the  $\text{PbZrO}_3$  phase at higher temperatures supports faster achievement of the equilibrium state. The tetragonal PZT phase reacts with  $\text{PbO}$  from  $\text{PbZrO}_3$  and following with created a  $\text{PbO}$  deficient  $\text{PbZrO}_3$  phase in which  $\text{Zr}$  ions have higher chemical activity. In XRD records of mixtures (1) and (2) after thermal treatment, the peak from (partial Ti substituted)  $\text{PbZrO}_3$  phase can be visible but it has lower intensity

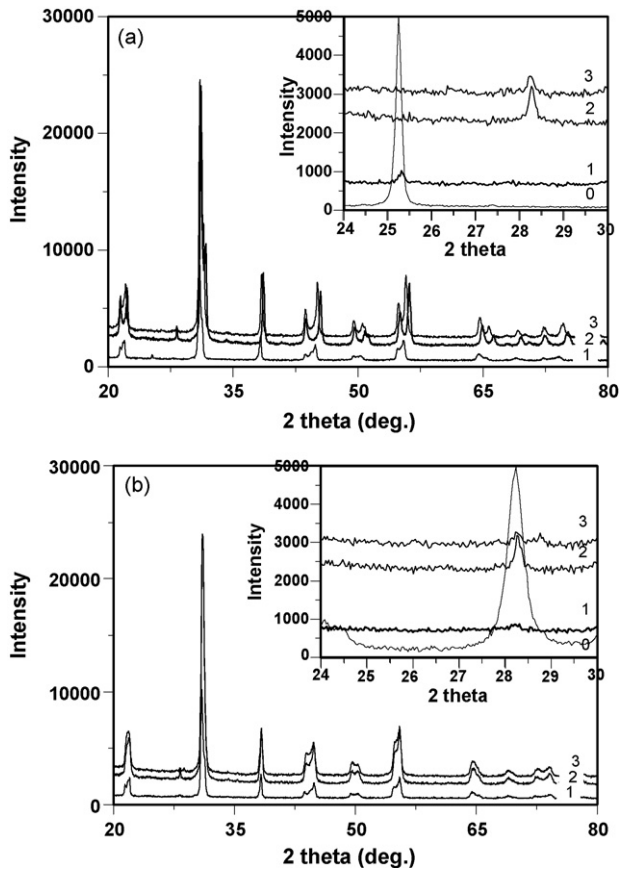


Fig. 6. XRD diffraction spectra of mixtures  $\text{Pb}(\text{Zr}_{0.53}\text{Ti}_{0.47})\text{O}_3$  calcinate with 2 or 5 wt.% excess of  $\text{TiO}_2$  (a) and  $\text{ZrO}_2$  (b). (0) pure  $\text{TiO}_2$  ( $\text{ZrO}_2$ ); (1) starting mixtures with 2 wt.% oxide excess; (2) mixtures with 5 wt.% oxide excess after sintering at  $1200^\circ\text{C}$ ; (3) mixtures with 2 wt.% oxide excess after sintering at  $1200^\circ\text{C}$ .

and it is worse distinguished from the background in mixture (1). The same phase (Fig. 5e) was found in final PZT ceramics after sintering of the PZT mixture composed from tetragonal and rhombohedral PZT phases but with  $x=0.55$  (double content of the rhombohedral phase than in mixture (1)). From above result, the formation of this phase is probably related to the presence of rhombohedral  $\text{PbZr}_{0.6}\text{Ti}_{0.4}\text{O}_3$  or  $\text{PbZrO}_3$  phase in the mixtures. Note that this phase was not observed in the XRD spectrum of PZT calcinate ( $x=0.53$ ) after the same thermal treatment. Thus, the reason for Ti and Zr ion diffusion between various interacting PZT phases with the formation of the final PZT solid solution are differences in chemical activities of Ti and Zr ions in these phases. Chemical activities of Ti and Zr ions are significantly influenced by inequality in  $\text{PbO}$  partial pressures between rhombohedral phase and tetragonal PZT phases, which causes the creation of  $\text{PbO}$  deficient PZT phase.  $\text{PbO}$  vapour (from rhombohedral or  $\text{PbZrO}_3$  phases with higher  $\text{PbO}$  partial pressure than in tetragonal phase) interacts with tetragonal phase and following smaller and more reactive Ti ions diffuses faster than Zr ions into the lattice of tetragonal phase from  $\text{PbO}$  deficient nonstoichiometric rhombohedral phase (besides,  $\text{TiO}_2$  is more soluble in  $\text{PbO}$  in comparison with  $\text{ZrO}_2$ ). This effect supports tendency to preserve of the tetragonality of major tetragonal phase (70 at.% in mixture (1)) in ceramics. The decrease in con-

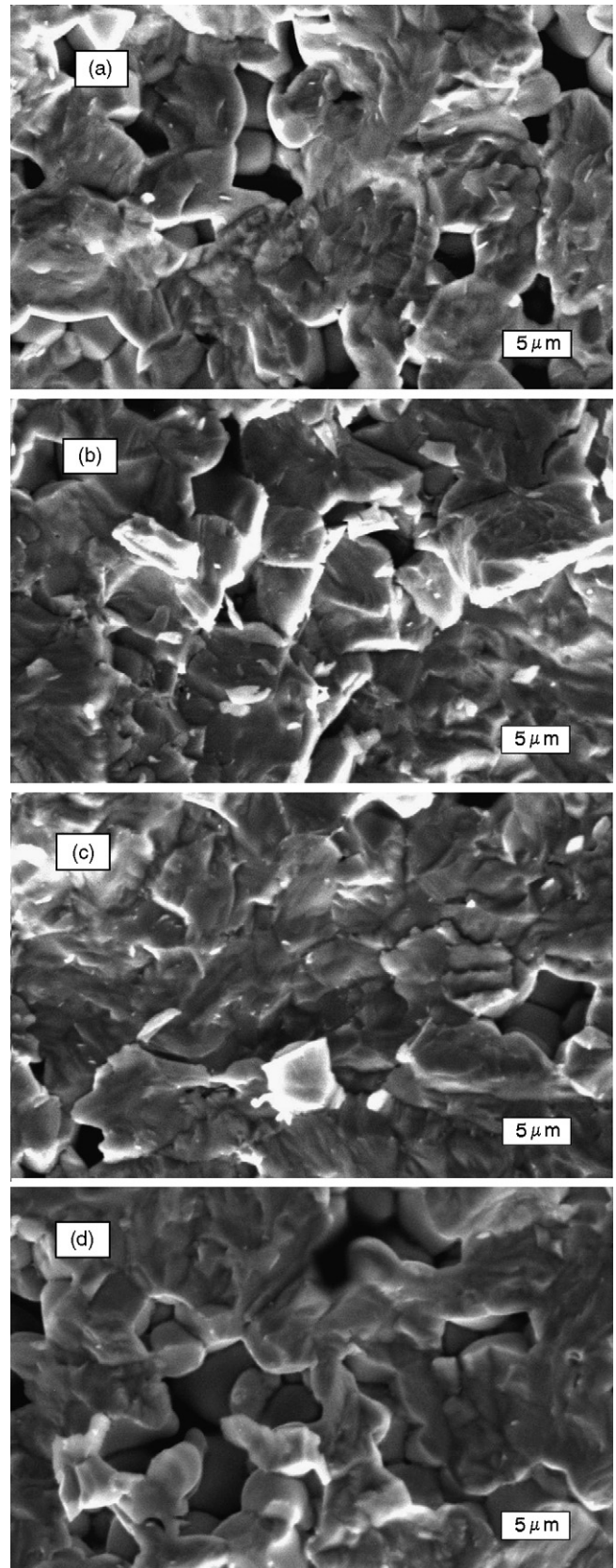


Fig. 7. Microstructures of fractured PZT ceramic samples prepared from  $\text{Pb}(\text{Zr}_{0.53}\text{Ti}_{0.47})\text{O}_3$  calcinate (a), mixture (1) (b), mixture (2) (c), mixture (3) (d).

centration of Ti ions in original rhombohedral phase causes the rise in PbO partial pressure again. The residual low reactive Zr ions interact with PZT phase (as  $ZrO_2$  or in the form of nonstoichiometric rhombohedral phase) in last stage of process. High interaction rate and diffusion of PbO or  $TiO_2$  into PZT phase can be seen in XRD spectrum of mixture (composed from PZT rhombohedral and  $PbTiO_3$  phases) with  $\Delta x = 0.07$  (the highest used deviation from final equilibrium stoichiometry) after thermal treatment. The absence of peaks from  $PbZrO_3$  phase, pure PbO or  $TiO_2$  phases (Fig. 4d) and very low fraction of rhombohedral phase (its presence verifies very small broadening of peaks from reflections of (1 1 1) and (2 0 0) planes of tetragonal phase only) in final PZT system ( $x = 0.53$ ) confirm diffusion of PbO and  $TiO_2$  from  $PbTiO_3$  phase to PZT phase. The rate determining process for the formation of equilibrium stoichiometric PZT systems created by the interaction of PZT phases are differences in PbO partial pressures of individual phases, the low chemical activity and diffusion rate of Zr ions into lattice of PZT perovskite phases. The similar conclusion was found in Ref. 18 which shows that  $PbTiO_3$  phase is formed in the first stage of calcination of oxide mixtures (PbO,  $TiO_2$  and  $ZrO_2$ ) and residual PbO, respectively,  $ZrO_2$  (only very low amount of  $PbZrO_3$  was found) interact in next stage with creation of final PZT system.

#### 4. Conclusions

The results of experimental work can be summarized in the following points:

1. In PZT systems prepared by the calcination of oxide mixtures, the rise of lattice parameter  $a$  and the decrease in parameter  $c$  of tetragonal phase was observed. The biphasic PZT system was found in PZT ceramic prepared by the sintering of PZT calcinate with  $x = 0.53$ .
2. The  $Pb(Zr_{0.53}Ti_{0.47})O_3$  systems prepared by sintering of perovskite mixtures had tetragonal symmetry without the presence of rhombohedral phase.
3. In XRD spectra of PZT mixtures after fast thermal treatment at  $780^\circ C$ , a small peak from  $PbZrO_3$  phase phase was visible. This phase was not observed in XRD spectrum of thermal treated PZT calcinate with  $x = 0.53$ .
4. Excess  $TiO_2$  intensively interacts with  $Pb(Zr_{0.53}Ti_{0.47})O_3$  phase and  $TiO_2$  is substituted for  $ZrO_2$ , which is excluded from this phase. On the other hand, the excess  $ZrO_2$  with given phase does not react.
5. The magnitude of deviation from equilibrium chemical composition or fluctuation from final stoichiometry in PZT phase in starting powder perovskite mixtures are not crucial for the formation of monophase  $Pb(Zr_{0.53}Ti_{0.47})O_3$  ceramic system (with composition close to morphotropic phase boundary) prepared by the interaction of perovskite phases.

#### Acknowledgements

This work was supported by the Slovak Grant Agency of the Ministry of Education of the Slovak Republic and the Slovak Academy of Sciences, Project No. 2/5145/25.

#### References

1. Jaffe, B., Cook, W. R. and Jaffe, H., *Piezoelectric Ceramics*. Academic Press, London, 1971.
2. Noheda, B., Cox, D. E., Shirane, G., Gonzalo, J. A., Cross, L. E. and Park, S. E., A monoclinic ferroelectric phase in  $Pb(Zr_{1-x}Ti_x)O_3$  solid solution. *Appl. Phys. Lett.*, 1999, **74**(14), 2059.
3. Noheda, B., Cox, D. E., Shirane, G., Guo, R., Jones, B. and Cross, L. E., Stability of the monoclinic phase in the ferroelectric perovskite  $PbZr_{1-x}Ti_xO_3$ . *Phys. Rev.*, 2000, **B63**, 014103-1.
4. Cao, W. and Cross, L. E., Theoretical model for the morphotropic phase boundary in lead zirconate–lead titanate solid solution. *Phys. Rev.*, 1993, **B47**(9), 4825.
5. Benguigui, L., Thermodynamic theory of the morphotropic phase transition tetragonal–rhombohedral in the perovskite ferroelectrics. *Solid State Commun.*, 1972, **11**, 625.
6. Isupov, V. A., *Soviet Solid State Phys.*, 1976, **18**(4), 921.
7. Ari-Gur, P. and Benguigui, L., Direct determination of the coexistence region in the solid solutions  $Pb(Zr_{1-x}Ti_x)O_3$ . *J. Phys. D: Appl. Phys.*, 1975, **8**, 1856.
8. Soares, M. R., Senos, A. M. R. and Mantas, P. Q., Phase coexistence region and dielectric properties of PZT ceramics. *J. Eur. Ceram. Soc.*, 2000, **20**, 321.
9. Kakegawa, K., Mohri, J., Takahashi, T., Yamamura, H. and Shirasaki, S., A compositional fluctuation and properties of  $Pb(Zr,Ti)O_3$ . *Solid State Commun.*, 1977, **24**, 769.
10. Wilkinson, A. P., Xu, J., Pattanaik, S. and Billinge, S. J. L., Neutron scattering studies of compositional heterogeneity in sol–gel processed lead zirconate titanates. *Chem. Matter*, 1998, **10**, 3611.
11. Brunckova, H., Medvecký, L. and Briancin, Influence of hydrolysis conditions of the acetate sol/gel process on the stoichiometry of PZT powders. *Ceram. Int.*, 2004, **30**, 453.
12. Kakegawa, K., Matsunga, O., Kato, T. and Sasaki, Y., Compositional change and compositional fluctuation in  $Pb(Zr,Ti)O_3$  containing excess PbO. *J. Am. Ceram. Soc.*, 1995, **78**(4), 1071.
13. Fernandes, J. C., Hall, D. A., Cockburn, M. R. and Greaves, G. N., Phase coexistence in PZT ceramic powder. *Nucl. Instrum. Meth. Phys. Res.*, 1995, **B97**, 137.
14. Boutarfaia, A., Boudaren, C., Mousser, A. and Bouaoud, S. E., Study of phase transition line of PZT ceramics by X-ray diffraction. *Ceram. Int.*, 1995, **21**, 391.
15. Boutarfaia, A., Investigations of co-existence region in lead zirconate–titanate solid solutions: X-ray diffraction studies. *Ceram. Int.*, 2000, **26**, 583.
16. Hunter, B. A. and Howard, C. J., *LHPM—A Computer Program for Rietveld Analysis of X-ray and Neutron Powder Diffraction Patterns*. Lucas Heights Research Laboratories, Australia, 2000.
17. Moulson, A. J. and Herbert, J. M., *Electroceramics*. Chapman & Hall, London, 1990, p. 283.
18. Chandratreya, S. S., Fulrath, R. M. and Pask, J. A., Reaction mechanisms in the formation of PZT solid solutions. *J. Am. Ceram. Soc.*, 1981, **64**, 422.
19. Hammersley, A. P., Svensson, S. O., Hanfland, M., Fitch, A. N. and Häuselmann, D., Two-dimensional detector software: from real detector to idealised image or two-theta scan. *High Press. Res.*, 1996, **14**, 235.